



Optimizing Unconventional Reservoir Performance in Niger Delta: A 3D Geostatistical driven Geomechanics Evaluation-Integrated Approach to Characterization

*Osaki, L.J., Onwubuariri, C.N., Agoha, C.C

1(Department of Physics and Geology, Federal University Otuoke, Bayelsa State, Nigeria)

2(Michael Okpara University of Agriculture Umudike, Nigeria)

2(Department of Geology, Federal University of Technology Owerri, Imo State, Nigeria)

Abstract: This work efficiently incorporated geomechanical characteristics into a 3-D geostatic model of a reservoir in the Niger Delta basin, Nigeria, for the assessment of deformability and rock strength utilizing well logs and 3D seismic data. Unconsolidated sandstone and compacted shale were characterized and assessed through the determination of elastic moduli (Poisson ratio, Young's modulus, Bulk modulus and Shear modulus) and Unconfined Compressive Strength (UCS) utilizing sonic logs and petrophysical analysis. Correlations and cross plots were employed to compare the evaluated reservoir strength and physical properties (including modulus, porosity, and velocity) of the five delineated zones from five vertical wells in the studied reservoir for validation purposes. The integration of elastic characteristics and unconfined compressive strength into the 3D static model of the analyzed reservoir was executed to account for significant lateral variability of rock elastic moduli and strength in zones lacking well control, particularly from the well points. The findings indicate that the average parameters of the poorly cemented sand exhibit a decreased Poisson ratio, Young modulus, Bulk modulus, Shear modulus, and Unconfined compressive strength (0.26, 2.1GPa, 11.05GPa, 7.21GPa, and 13.91MPa, respectively), with elevated porosity (0.25). Conversely, the compacted shale exhibits increased Poisson ratio, Young modulus, Bulk modulus, Shear modulus, and rock strength, quantified as 0.37, 17.95GPa, 20.79GPa, 52.92MPa respectively, with reduced porosity, measured at 0.06. A significant enhancement in rock strength and elastic moduli occurs with a corresponding reduction in porosity. The mechanical failure in the NNW direction of the reservoir will be comparatively less severe than in other zones, as analyzed using the 3D earth model. This research will yield valuable information that will facilitate the management of reservoir stress and strain throughout development, optimize reservoir performance, and reduce risk.

Keywords: Poisson ratio, Young modulus, Bulk modulus, Shear modulus unconfined compression strength and Niger delta

1. Introduction

Technological revolution is at the heart of deepwater oil operations, allowing us to explore, drill and produce oil in some of the world's most challenging environments. In contrast to conventional reservoirs, unconventional reservoirs have heightened geological complexities that complicate drilling and well design, resulting in increased drilling time, production cost, and operational risk. The nature of these operations is influenced by factors such as faulting and fracturing, which could result in unstable wellbores, lost circulation, and challenges in accessing the target reservoir. Additionally, heterogeneous rock properties, including variations in porosity, permeability, and rock strength, can impact drilling rates, wellbore stability, and reservoir performance. Besides the problems of drilling and well placement, evaluating the distribution, volumetric, and net-to-gross ratio of the



unconventional reservoir is a significant obstacle. The complicated compartmentalization of the reservoir makes its production much more expensive, and it is only sustainable if there exists a substantial reserve that can support exploitation over a prolonged period. Nonetheless, unconventional reservoirs may provide greater long-term profitability compared to conventional reservoirs because they are closer to the surface and have increase longer depletion span. The need for unconventional hydrocarbon sources remains necessary, since their availability facilitates production growth and reduces dependence on conventional crude oil production.

Understanding the geomechanics of a hydrocarbon field is essential for the optimal economic exploitation of an unconventional reservoir. Geomechanical issues, including pore pressure prediction, fault/seal integrity, well stability, permeability heterogeneity assessment, and sand production forecasting, benefit from precise measurement and evaluation of geomechanical parameters. Predicting safe and economical operation depends critically on a thorough knowledge of the stress state and fluid-rock interaction conditions in porous media before different scenarios including drilling, stimulation, and production of hydrocarbon reservoirs. The paramount significance resides in assessing the three-dimensional spatial distribution of geomechanical properties and petrophysical parameters at the reservoir scale within such a challenging environment. Consequently, the 3D seismic-driven geomechanical model will increase the knowledge of the complicated geometry, presenting precise scaling and proportional identification and quantification of essential reservoir properties, including porosity, permeability, fluid saturations, lithology, and geomechanical properties. These characteristics determine the reservoir's capacity to store and produce hydrocarbons, affecting productivity, recovery efficiency, and economic viability [33].

The reservoir's 3D static geological model includes a 3D volume structure [9,46,47,48]. A three-dimensional static model of the reservoir defines the structure, stratigraphy, and rock characteristics at a given time [3,47]. One of the most difficult aspects of reservoir modeling is accurately representing reservoir geometry, such as the structural framework and precise stratigraphic strata [35,41]. The static reservoir model is built from many data sources, including well logs, cores, well testing, and production data [12]. The reservoir model is created in two stages: construction modeling and petrophysical modeling, in which geostatistical techniques distribute reservoir features across the reservoir structure [16]. Geostatistical approaches such as deterministic (such as Kriging) and stochastic (such as Sequential Gaussian Simulation) methods are often used to develop reservoir models [47, 48] A reservoir model plus a geomechanics model make up the static reservoir geomechanical modeling system. As stated, geostatistical approaches can be used to develop the static reservoir model. Furthermore, the geomechanical characteristics model can be built using geostatistical approaches in the same way that the static reservoir model is modelled. Numerical modeling, particularly the reservoir geomechanical model, is a dependable tool that integrates diverse data, including geological, geophysical, and engineering data, to analyze multiple scenarios over the reservoir's lifespan [14,22,25,45,18]. A 3D seismic-driven geomechanical model is an outstanding tool for evaluating temporal and lateral variations in petrophysical and mechanical parameters, particularly in complex, heterogeneous, and unconventional reservoirs.

The dependability of seismic-derived elastic characteristics and pore pressure is intrinsically connected to the precision of seismic velocities [11,39]. Seismic data provides critical information on the structure, stratigraphy, petrophysical, and geophysical features of the subsurface, which may be examined to derive significant elastic mechanical parameters of the reservoir rock. Initially, the seismic data must be calibrated using well logs and, if feasible, with core data to enhance its predictive efficacy. The seismic data will thereafter be inverted using suitable inversion software. Well logs have shown significant use in predicting elastic geomechanical characteristics, particularly due to the availability of many crucial empirical equations that correlate distinct elastic rock moduli with the Lamé parameters. Logs such as sonic, density, resistivity, and gamma are valuable for calculating the elastic characteristics of rock.

A comparable study on Geomechanical Characterization was conducted in Wabamun Lake and the Nisku formation in Canada by [45,47], utilizing core samples and a 2D methodology, although with the constraint of oversimplifying geological structures. This study employs a 3D seismic-driven geomechanical model technique to thoroughly analyze and integrate the geomechanical properties of a reservoir into a 3D earth model, using well logs and seismic sections to map and interpolate changes in rock deformability and strength. Cross plots and correlation analyses of rock mechanical characteristics and petrophysical parameters were conducted to validate their connection; nevertheless, reserve calculation and reservoir producibility are outside the scope of



this study. Rock strength and other characteristics are derived from data acquired via well logs, since most variables influencing rock strength concurrently impact elastic modulus and petrophysical parameters ascertainable from geophysical measurements [23,24]. More accurate reservoir models and better reservoir management methods follow from a thorough knowledge of reservoir properties and heterogeneities made possible by the integration of petrophysical and geomechanical study in 3-D model utilizing geostatistical simulation techniques. Thus, the objective of this study is to evaluate Poissons ratio, Bulk modulus, young modulus, Shear modulus, compressibility, unconfined compressive strength (UCS) and porosity of a deep-water reservoir in the Niger Delta using well-log data. The advantages for more precise well and field development planning in structural complicated reservoir like the Niger Delta basin will be shown by the synergy of 3D geological model with mechanical parameters and rock strength. This will minimize downtime, enhance production efficiency, improve overall production, and maximize return rate of economic assets.

2. Theoretical Background

Two petrophysical logs that are crucial for predicting geomechanical parameters and characterizing reservoirs are density and sonic (both compressional and shear waves) [20]. Dynamical properties are geomechanical parameters that are computed using petrophysical logs. An estimate of the geomechanical characteristics throughout the reservoirs, not only the tested depths, is obtained by determining the dynamic properties.

Compressional and shear wave velocity

Practically every equation that has been presented for determining rock strength and elastic moduli from geophysical logs uses either compressional velocity (V_p), transit time ($\mu\text{s/m}$), or porosity, according to [7,23,24,29,32]. Lithology, interstitial fluid, porosity, clay content, depth, density, temperature, and other elements all have an impact on seismic velocities. Lithology influences velocity (P-wave and S-wave). The velocity at which acoustic waves penetrate rocks is influenced by porosity since pores are among the weakest and most deformable parts of rocks [8, 9]. In 1950, Wyllie et al. created equations that demonstrated the connection between porosity and velocity.

$$\Delta t = \phi \Delta t_f + (1 - \phi) \Delta t_{ma} \quad (1)$$

where $\Delta t, \Delta t_f, \Delta t_m$ = specific transit time (slowness), pore fluid, rock matrix respectively, ϕ = Porosity

In terms of velocity, equation (10) can be re-written as:

$$\frac{1}{v} = \frac{\phi}{v_f} + \frac{(1 - \phi)}{v_{ma}} \quad (2)$$

where, v = Bulk density v_f = Velocity of the fluid v_{ma} = Velocity of rock matrix.

Shear and compressional wave velocities are other properties of reservoirs that should be properly determined. Equation may be used to determine the compressional wave velocity based on the travel time obtained from sonic logs. (1):

$$V_p = 1/DT \quad (3)$$

V_p denotes the compressional wave velocity, whereas DT represents the compressional wave travel time. For zones where travel time was unrecorded, DT was approximated using density travel time correlation and porosity data. Several correlations have been established to estimate shear wave velocity, like the calculation of compressional wave velocity. These include the Han correlation [21], Castagna correlation [8] Multiple regression method [2] and Brocher correlation [5,6], as detailed in Table 1, where V_s and V_p denote shear and compressional wave velocities, respectively. $NPHI$ denotes neutron porosity, whereas $RHOB$ represents density.

Table 1: Proposed correlations for shear wave velocity calculation

	Correlation	Eq. no
Han correlation	$V_s = 4060 - 6280\phi$	4
Castagna correlation	$V_s(\text{km/s}) = -0.05509 V_p^2 + 1.0168V_p - 1.0305$	5
Multivariate model	$V_s = 17.0885 + 0.4068 \times V_p - 2.1907 \times NPHI^2 \times 1.1794 - NPHI - 3.2747 \times RHOB^2 + 15.3587 \times RHOB$	6



Brocher
correlation

$$V_s = 0.7858 - 1.2344 \times V_p + 0.7949 \times V_p^2 - 0.1238 \times V_p^3 + 0.0064 \times V_p^4$$

7

Petroleum Geology of the Study Area

The research location, the oil-rich Niger Delta region, is situated within the offshore depo belt of the Niger Delta basin in Nigeria (Figure 2). This sedimentary basin is characterized by a clastic environment mostly composed of sands and shales. The Niger Delta Province encompasses a singular recognized petroleum system known as the Tertiary Niger Delta (Akata-Agbada) Petroleum System. The region is a sedimentary basin, with three primary formations: Akata, Agbada, and Benin Formations. The Akata consists of dense shale formations and functions as a prospective source rock. It is considered to have originated due to the movement of terrestrial organic materials and clays to deep seas during the beginning of the Paleocene. The thickness of this deposit is believed to be around 7,000 meters, and it is situated under the whole delta with significant overpressure. The Agbada Formation serves as the principal oil and gas resource of the delta. It functions as a transition zone and comprises an intercalation of sand and shale (paralic siliciclastics), with a thickness of 3700 meters, representing the deltaic segment of the Niger Delta sequence. The Agbada Formation is overlain by the Benin Formation. The Benin Formation consists of sands around 2000 meters in thickness [27].

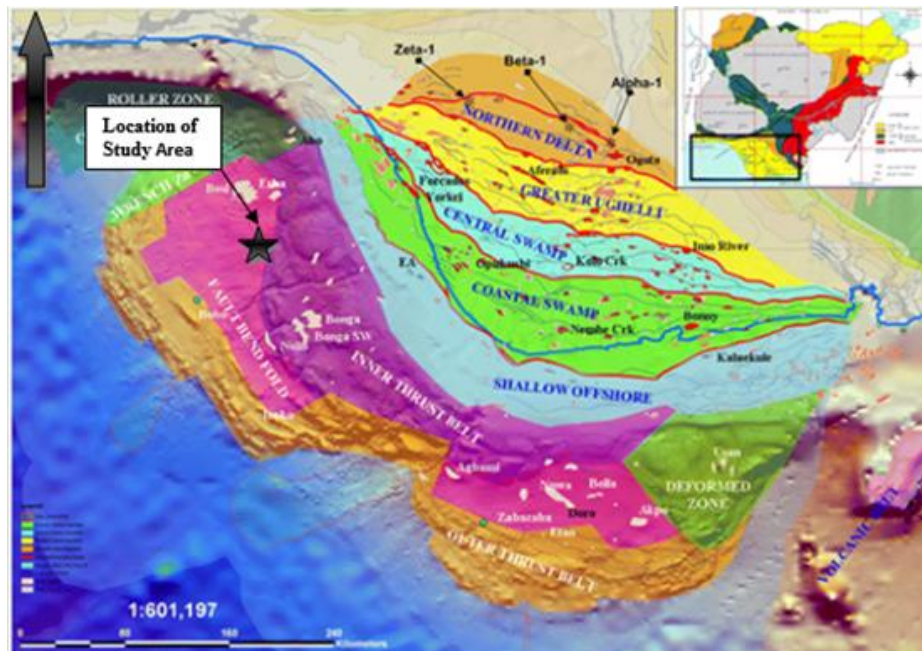


Figure 1: Map of the Niger Delta Basin showing Study Area (Onuorah et al., 2014).

3. Materials and Methods

The material used for this work consists of digitize conventional logs (GR, Sonic, Resistivity, Compensated Density, and Neutron Porosity Logs) in LAS format, digitize 3D seismic data (in Seg-Y data format), Check shots, Schlumberger Petrel, interactive petrophysics, and MS Excel software for the analyses and interpretation of these data. Core samples of the reservoir's overburden formation are not readily available for geomechanical laboratory testing in this project, hence the assessment of the 3D earth mechanical property model is based on data gathered from well logs and 3D seismic volume.

Seismic interpretation and petrophysical analysis.

Detailed 3D seismic interpretation and petrophysical analysis were carried out using the Schlumberger Petrel. This includes loading available data (seismic and logs) into the software, generating a synthetic seismogram to determine the horizons or picks of interest to be interpreted on the seismic profile, fault and horizon interpretation, creation of fault polygons, zapping/interpolation/smoothing of horizons, generation of depth converted contour maps, and generation of geomodels. The Petrel software was used to verify data at the time of input to ascertain its compliance with the dataset's minimum and maximum limits. The availability and



uniformity of the GR and Sonic logs for all five wells were identified as vital for lithological delineation and compression velocity generation; the logs were standardized to prevent erroneous readings. Three-dimensional seismic data and well log data were used for stratigraphic correlation and reservoir structure identification. This was accomplished by highlighting surfaces of interest from the five wells on a well correlation panel. The reservoir's boundary and geometry were defined using seismic data. This facilitated the assessment of the reservoirs' geometry both laterally and in depth. The 3D seismic volume served as the basis for constructing the 3D geomechanical models of the reservoirs.

The 1D and 3D reservoir geomechanics modeling

The 1D geomechanical and 1D petrophysical (reservoir) properties modeling are two components of the one-dimensional modeling of reservoir geomechanics. We use log data from the five wells to analyze 1D petrophysical and geomechanical parameters. By calculating the elastic moduli (Poisson ratio, Young modulus, Bulk modulus and Shear modulus) and the unconfined compressive strength (UCS) using sonic logs and petrophysical analysis, 1D geomechanical modeling provides a continuous numerical representation of geomechanical properties. Upscaling the well log, interpreting the data, geocell modeling, and petrophysical modeling are the steps involved in the study of petrophysical and geomechanical data. The 3D geomechanical model and the 3D static reservoir model are two components of the three-dimensional modeling of reservoir geomechanics. Each model includes 3D structural and property representations of the reservoir's geology, structure, stratigraphy, sublayers, and faults. The high-resolution structural/geological model is used to construct the 3D static geomechanical model. Geostatistical techniques based on the 1D geomechanical models from the log data are used to distribute the 3D geomechanical properties. The 3D geomechanical model is filled using geostatistical techniques like the Kriging and Gaussian (Sequential Gaussian Simulation (SGS)) approaches. To capture significant lateral variation of rock elastic moduli and strength into locations where well control may not exist, particularly off the well locations, the mechanical and petrophysical parameters, rock strength, and structural characteristics were finally analyzed on a 3D geomechanical model of the reservoir. This shows the reservoir's structural limitations, rock strength, and lateral extent of deformability around the well environment.

Graphical analysis of petrophysical and geomechanical parameters

Cross plots were used to graphically analyze the connection between the estimated elastic moduli, unconfined compressive strength, and petrophysical characteristics. In terms of a formation rock strength (UCS), there is a definite correlation between its mechanical and petrophysical characteristics, according to [23,51]. The suggested relationship between the reservoir rock unconfined compressive strength and the geomechanical analysis that was assessed from the lithological units in the formation under study is justified in this work by a graphic report or cross plot. When required, the visual analysis of these cross plots would provide a foundation for compromise or a quality check, particularly in cases when statistical findings may be misleading.

Determination of Rock Geomechanical Properties

The mechanical parameters of the field were assessed using wireline logs. These elastic parameters include the Poisson ratio, young modulus (E), shear/rigidity modulus (G), bulk and matrix/grain moduli (K_b and K_m). Bulk and grain compressibility (C_b, C_r) Biots coefficient (a), and inelastic prosperity, unconfined compressive strength (UCS).

Young's modulus (E) is a measure of the property of the rock to resist deformation. It is the ratio of compressive/ tensile strength to compressive/tensile strains which for a rock that has similar properties and identical in all direction, homogenous, and elastic the modulus is given as:

$$E = \frac{9GK_b}{3K_b + G} \quad (8)$$

Poisson Ratio (ν)

The log-derived Poisson ratio was calculated from acoustic measurements, specifically the sonic log, which is typically presented in terms of slowness. This slowness is the reciprocal of velocity, represented as interval transit times (ΔT) measured in microseconds per foot. The ratio of the slowness of compressional waves (ΔV_p) to the slowness of shear waves (V_s) is utilized to calculate the Poisson ratio [34].



$$\nu = 0.5 \frac{\left[\left(\frac{V_p}{V_s} \right)^2 - 1 \right]}{\left[\left(\frac{V_p}{V_s} \right)^2 - 1 \right]} \quad (9)$$

The theoretical maximum value of ν is 0.5

Where V_p = compression wave velocity and V_s = shear wave velocity

Shear Modulus (G)

The Shear modulus is the ratio of the Shear stress to the Shear strain which for a homogeneous and elastic rock is given by equation (13) [43].

$$G = \frac{a\rho_b}{\nu(\Delta T_s)} \quad (10)$$

Where coefficient $a = 13464$, ρ_b = Bulk density in g/cm^3 , ΔT_s = Shear sonic transit time in us/m . ν = Poisson ratio. The unit of G is 10^6 MPa.

Bulk Modulus (K_b) is a static modulus but an equivalent dynamic modulus can be computed from the sonic and density logs. The relationship is given in below:

$$K_b = a\rho_b \left(\frac{1}{\Delta T_c^2} - \frac{4}{3T_s^2} \right) \quad (11)$$

where coefficient $a = 13464$, ρ_b = Bulk density in g/cm^3 , ΔT_c and ΔT_s = change in compression and shear wave respectively in us/m . The unit of K_b is 10^6 MPa.

Unconfined compressive Strength (UCS) and Porosity(ϕ)

Of the various empirical relationships suggested for sandstone, shale, and limestone rocks, equation (12) is most applicable to fine-grained, both consolidated and unconsolidated sandstones across all porosity ranges in the Niger Delta basin, while equation (13) for shales was utilized for comparative analysis.

Table 2: Relations between UCS and porosity in reservoir rocks

Lithology	Relationship Formula	Applicable Conditions	Eq. no
Sandstone	UCS = 277 exp(-10 ϕ)	2MPa < UCS < 360MPa ; 0.002 < ϕ < 0.33	12
Shale	UCS = 1.001 ϕ - 1.143 UCS > 79MPa ; ϕ < 0.1	UCS > 79MPa ; ϕ < 0.1	13
Limestone	UCS = 135.9 exp(-4.8 ϕ)	10MPa < UCS < 300MPa ; 0 < ϕ < 0.2	14

Volume of Shale

The volume of shale is the Bulk volume of the reservoir composed of clay minerals and clay bound water. V_{shale} was determined using Larinov (1962) equation (15)

$$V_{shale} = 0.083(2^{3.71I_{gr}} - 1)[Larinov, 1962] \quad (15)$$

Where I_{gr} is the shale index (gamma ray index) which is defined in (16)

$$I_{gr} = \frac{GR_{log} - GR_{min}}{GR_{max} - GR_{min}} \quad (16)$$

Where, GR_{log} = measured gamma ray log reading at depth (z), GR_{min} minimum gamma ray log in clean sand, GR_{max} = maximum gamma log reading (in clean shale) V_{shale} volume of shale in the formation at depth z .



Porosity

Porosity is the total volume of a rock occupied by pores both connected and unconnected. It is the ratio of the pore volume to the Bulk volume expressed as fraction %. Porosity is determined from density, sonic, neutron logs.

The total porosity was determined from density log data which are weighted average densities of the rock and pore fluid using equation

$$\theta_D = \frac{(\rho_{ma} - \rho_b)}{(\rho_{ma} - \rho_{fl})} \quad (17)$$

Where θ_D = total density porosity, ρ_{ma} density of rock matrix, ρ_b = measure density and ρ_{fl} = density of fluid.

Result Presentation

This section presents detailed results from the study, which include reservoir mapping, petrophysical evaluation, geomechanical analysis, graphical (cross plots) evaluation of rock strength against rock mechanical and petrophysical parameters and 3D geomechanical model analysis.

Reservoir Mapping

The first stage involved reservoir mapping through the delineation of five wells: OSA_01, OSA_02, OSA_03, OSA_04, and OSA_05 within a well correlation panel at depths of 9400ft to 9900ft. The evaluation of petrophysical properties and logs was conducted to determine the physical properties and quality of the reservoir in relation to its elastic properties and rock strength. Following careful geological examination of the five wells and correlation of the reservoir sand and shale sequences, the lithological and stratigraphic analysis of the reservoir utilizing GR log indicates that the geological units are primarily composed of sand and shale, showing an increasing trend in the sand/shale ratio. This confirms that the area of interest lies within the Agbada formation of the Niger Delta [19], as illustrated in Fig. 2. Differential subsidence variation from compaction of sediments and the presence of growth faults, as indicated in the Niger Delta [50], strongly control the lateral variation in reservoir thickness, which tends to be thickest at Law 004. The correlation showed five stacks of sand units in the reservoir, namely horizon A, B, C, D, E, and F across the five wells with thicknesses of approximately 82ft, 98ft, 104ft, 93ft, and 123ft respectively.

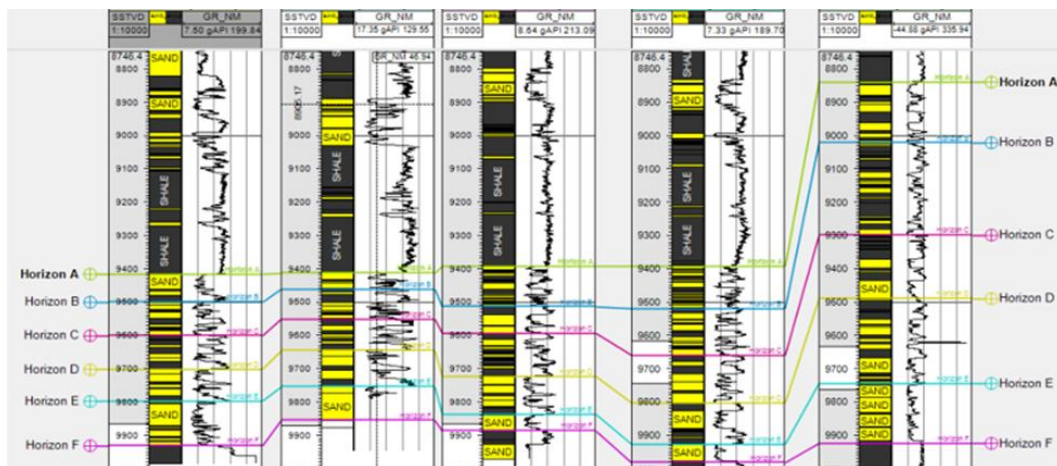


Figure 2: Well logs from well OSA_01, OSA_02, OSA_03, OSA_04, and OSA_05 showing delineated horizon of the studied reservoir using GR log

Determination of Petrophysical Properties:

A hydrocarbon reservoir is a subsurface rock characterized by effective porosity and permeability, typically containing economically viable quantities of hydrocarbons; these features are interrelated with mechanical and rock strength parameters [1]. The formation study involves using geophysical logs for evaluating various features of the reservoir. The clay content, porosity, water saturation, compressional velocity, and shear velocity influence the elastic moduli and rock strength of a reservoir. The porosity in this work was derived using density



data, the shale volume was inferred from GR data, and the compressional and shear velocities were computed using acoustic sonic data, as seen in Fig. 3. The petrophysical evaluation of the examined reservoir was essential as it confirms rock strength and predicts sand production analysis.

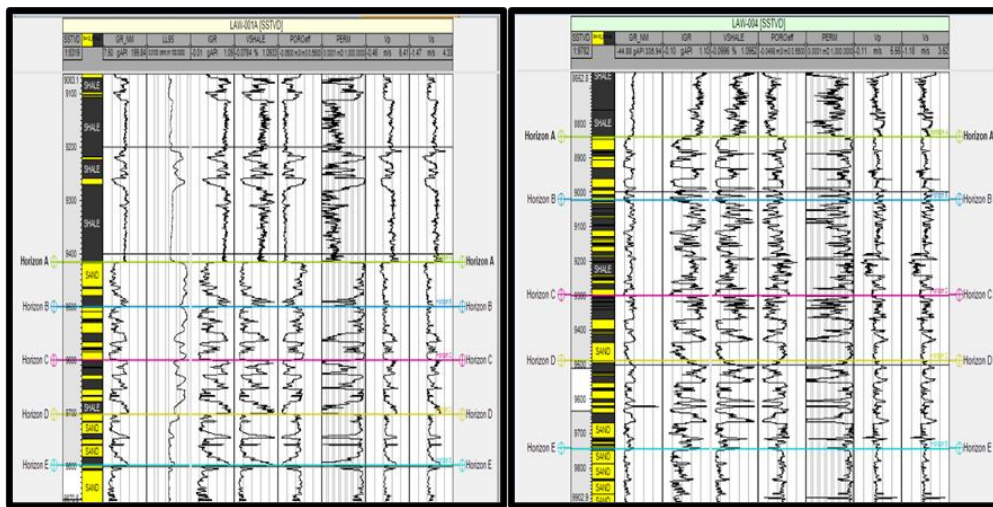


Figure 3: Petrophysical logs of OSA_01 and OSA_04 showing the physical properties of the reservoir rock as delineated with Gamma ray (GR), Resistivity (Ils) volume of shale (Vsh), compressional (Vp) and Shear velocity (Vs), and porosity

Determination of Geomechanical Parameters

The Poisson ratio, shear modulus, bulk modulus, Young's modulus and unconfined compressive strength of the five sand units intercalated with shale in the studied reservoir were computed at each well to determine the variation in sand and shale throughout the reservoir and the correlation between the elastic moduli and the rock strength of the formation under investigation. The geomechanical parameters were obtained by necessary empirical methods in Microsoft Excel and then loaded into Schlumberger Petrel software version 2013 to create and analyse mechanical property and unconfined compressive strength logs, as seen in Fig. 4 and Table 1.

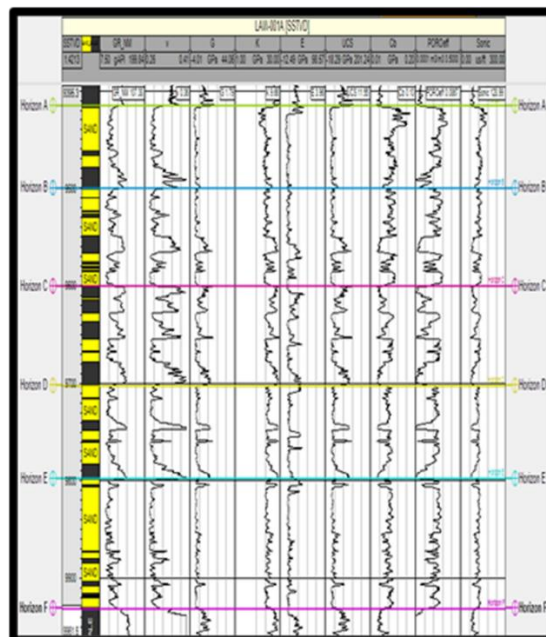


Figure 4: Lithological delineation with Poisson's ratio (ν), Bulk modulus (K), Shear modulus (G), Young modulus (E), the unconfined compression strength (UCS), Bulk compressibility (C_b), effective porosity, compression velocity (V_p) of the OSA_02.

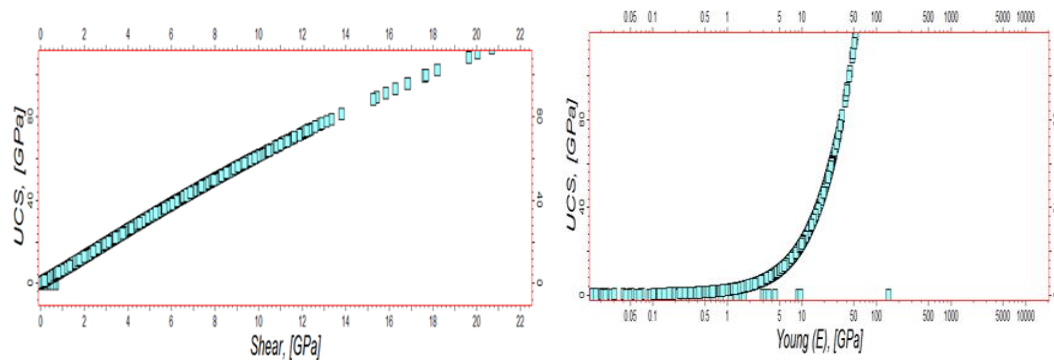


Table 3: Summary of Elastic Parameters, Porosity and Unconfined Compressive Strength for Sand and Shale Units of the Five Well of the Studied Reservoir.

Well	Parameter	Shale	Sand	Reservoir Sand Average	Reservoir Shale Average
OSA_01	Porosity (Ø)	0.04 – 0.07	0.21 – 0.26	0.24	0.06
	V	0.39 – 0.46	0.19 - 0.29	0.27	0.41
	G (Mpa)	7.98 – 9.10	834 – 18319	1.97	8.79
	E (Mpa)	20.09 - 22.09	5.90 - 7.80	6.50	21.09
	K (Mpa)	17.82 - 19.02	8.78 – 10.48	9.78	18.02
	UCS (Mpa)	54.83– 57.03	1.2 – 44.7	15.01	55.93
OSA_02	Porosity (Ø)	0.03 – 0.08	0.21 – 0.28	0.26	0.05
	V	0.21 – 0.36	0.23 – 0.38	0.24	0.38
	G (Mpa)	8.70 - 10.30	1.90 -2.53	2.10	9.10
	E(Mpa)	19.28 -21.28	6.00 – 7.31	6.22	20.98
	K (Mpa)	17.44 -19.14	9.78 – 11.10	10.21	18.34
	UCS (Mpa)	51.97 -59.62	13.20 -15.20	14.20	56.67
OSA_03	Porosity (Ø)	0.05 – 0.09	0.197 – 0.28	0.25	0.07
	V (Mpa)	0.21 – 0.29	0.23 – 0.38	0.25	0.36
	G (Mpa)	7.82 – 9.10	2.05 – 2.68	2.35	8.92
	E (Mpa)	20.73- 22.03	4.99 – 6.21	5.98	21.23
	K (Mpa)	17.92- 19.08	9.90- 11.04	10.10	18.52
	UCS(Mpa)	53.98- 56.44	12.58- 14.99	13.98	55.98
OSA_04	Porosity (Ø)	0.03 – 0.07	0.19 -0.23	0.22	0.05
	V	0.2 – 0.39	0.25 – 0.39	0.23	0.33
	G (Mpa)	7.67- 9.99	0.20- 0.31	0.22	8.87
	E (Mpa)	20.85- 22.00	5.50 – 7.88	6.57	21.35
	K (Mpa)	17.39 – 18.98	8.59- 11.02	9.99	18.33
	UCS (Mpa)	54.08 – 58.01	13.80 – 15.44	14.30	56.09
OSA_05	Porosity (Ø)	0.05 – 0.08	0.21-0.24	0.23	0.07
	V	0.12 – 0.35	0.14 – 0.47	0.26	0.39
	G (Mpa)	7.63- 9.97	0.22- 0.26	0.23	8.93
	E (Mpa)	19.43- 22.01	6.90- 8.66	7.20	20.99
	K (Mpa)	17.91- 19.34	9.44 – 12.02	10.30	18.11
	UCS (Mpa)	55.47- 57.22	13.27- 15.45	14.32	56.47

Cross Plots of Geomechanical Parameters, Rock Strength, Petrophysical properties and Depth

The proposed relationship between the unconfined compressive strength of the reservoir rock and the geomechanical parameters is substantiated by the graphic report or cross plot in this work, as indicated by [23,51]. The visual examination of these cross plots also provides a basis for compromise in situations where the statistical results may be misleading, such as when the cross plot clearly predicted low values while the statistical results in correlation rank high. The formation established a significant increase in unconfined compressive strength with Young modulus, Bulk modulus, and Shear modulus, as illustrated in Fig. 5. Conversely, the formation declared a decrease in unconfined compressive strength with Poisson ratio. To verify the relationship as depicted in Figs. 6, the increase in unconfined strength is a function of the decrease in porosity and acoustic travel time, cross plots of unconfined compression strength were also conducted against petrophysical parameters (porosity and acoustic travel time). The parameters' relationship with depth is illustrated in Fig 7, where the parameters increase as the depth increases.



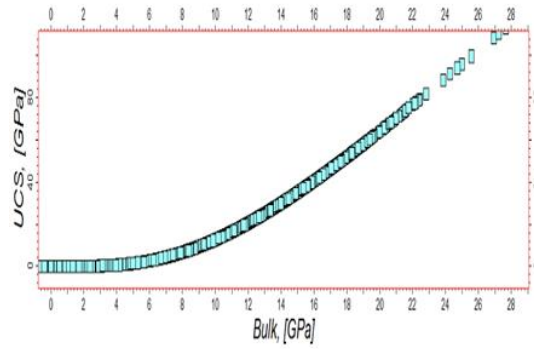


Figure 5: OSA_03 Cross-Plot Demonstrating the Correlation Between the Unconfined Compressive Strength (UCS) of the Reservoir Sand Units and the Shear Modulus, Young Modulus, and Bulk Modulus.

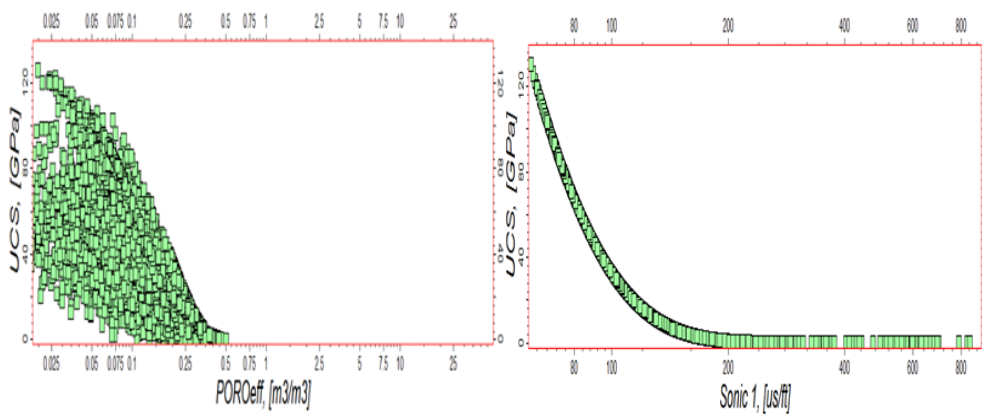


Figure 6: The relationship between the petrophysical parameters of OSA_02, which include porosity and acoustic sonic and the unconfined compressive strength (UCS) of the Reservoir Sand Units

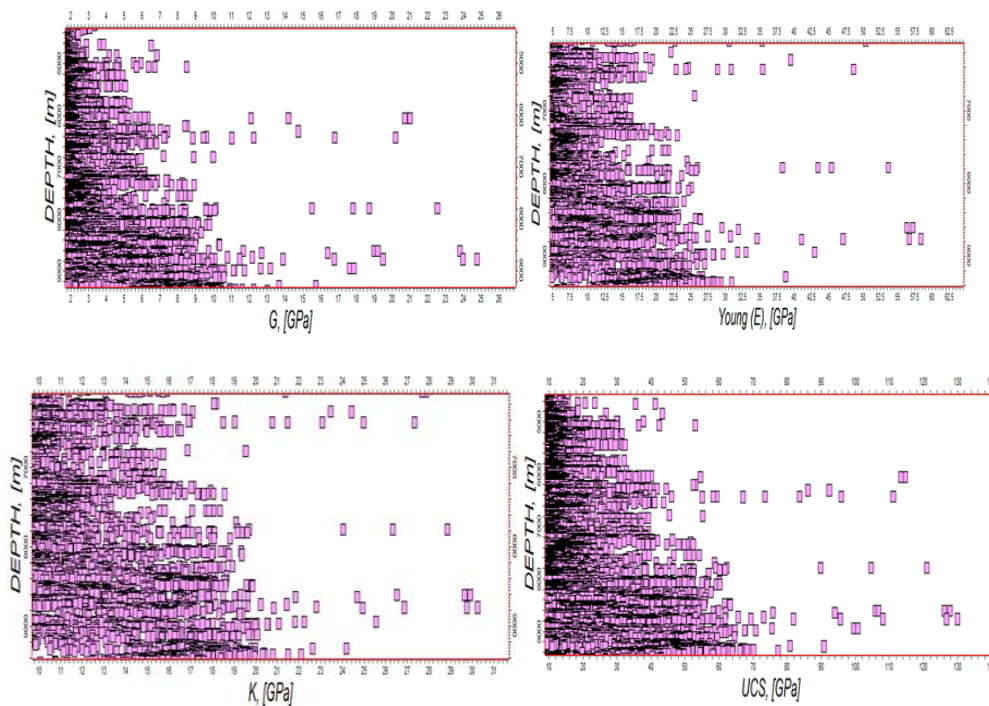


Figure 7: The relationship between depth, shear modulus, young modulus, bulk modulus, and unconfined compressive strength of the reservoir for OSA_05

Depth structure map and 3D geomechanical model of the researched reservoir:

A depth structure map was used to generate a south-west dipping (basinward) anticlinal structure of the study reservoir. This structure includes major faults (F1 & F2) and the various fault blocks depicted in Fig. 7. The northern and middle fault blocks represent the foot wall, while the southern fault block represents the hanging wall. A 3D mechanical earth model was created to depict the lateral distribution of the rock mechanical properties and rock strength (UCS) of the reservoir under investigation. The Poisson ratio, Young modulus, Shear modulus, Bulk modulus, and unconfined compressive strength (UCS) were simulated in a 3D static model of the studied reservoir to investigate the spatial variation of rock strength and deformity, as illustrated in the following figures.

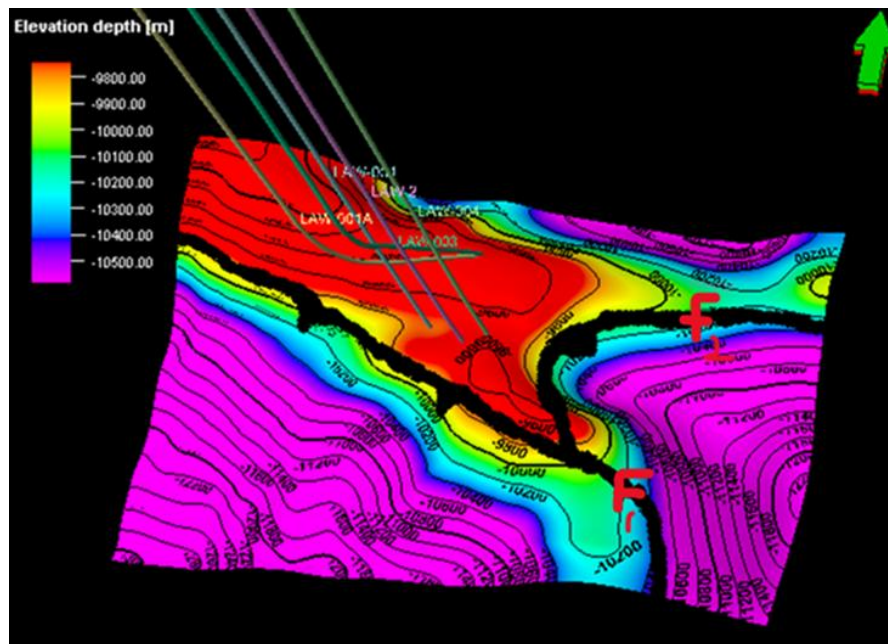


Figure 8: South-west dipping anticlinal structure with major faults and blocks displayed on the horizon A in the studied reservoir

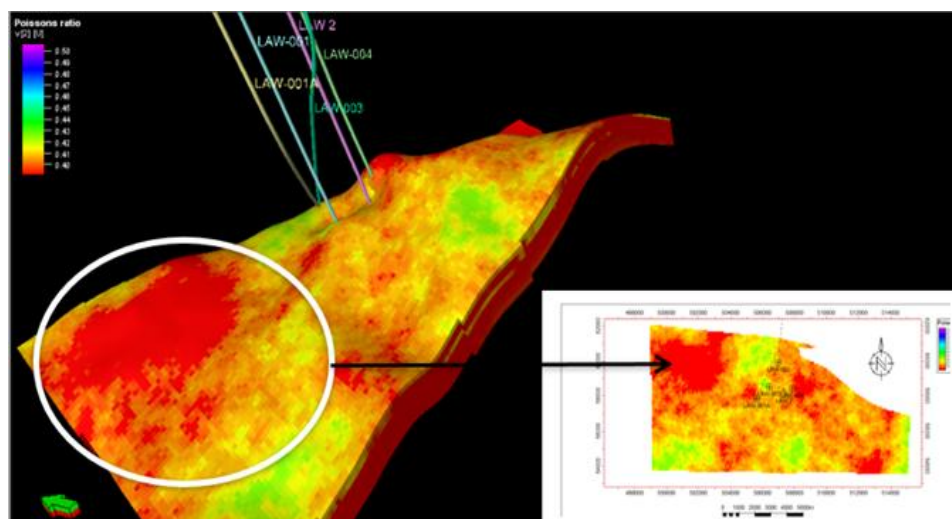


Figure 9: 3D Geologic model and penetrated wells with inserted map of studied reservoir showing spatial distribution of Poisson ratio with highest Poisson ratio zone on the reservoir top identified with a white circle in the northwest direction



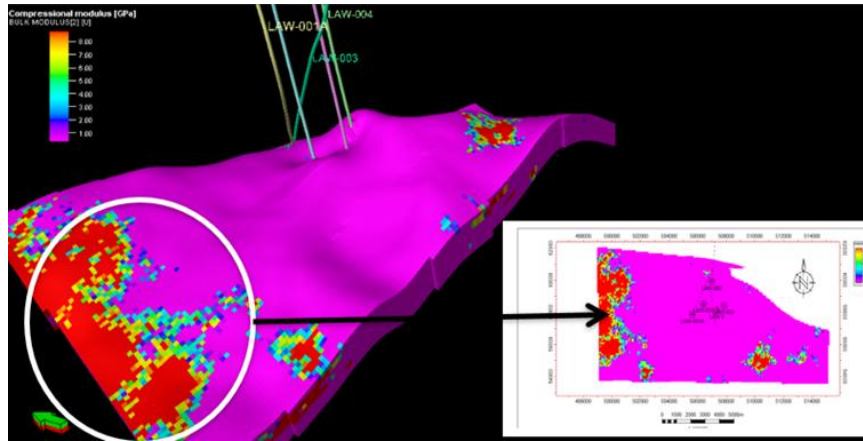


Figure 10: 3D Geologic model and penetrated well inserted map of the studied reservoir showing spatial distribution of Young modulus with highest Young modulus zone on the reservoir top identified with a white circle in the northwest direction.

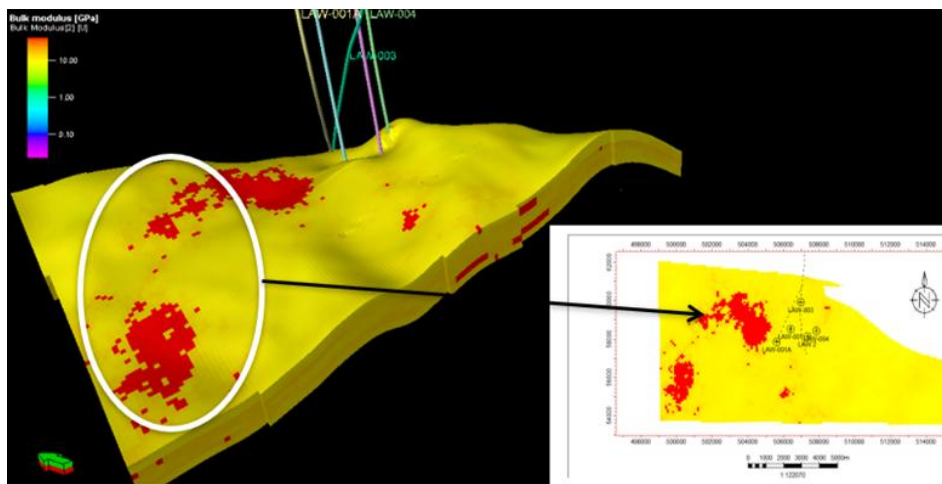


Figure 11: 3D Geologic model and penetrated wells with inserted map of studied reservoir displaying spatial distribution of Bulk modulus with highest Bulk modulus zone on the reservoir top identified with a white circle in the northwest direction

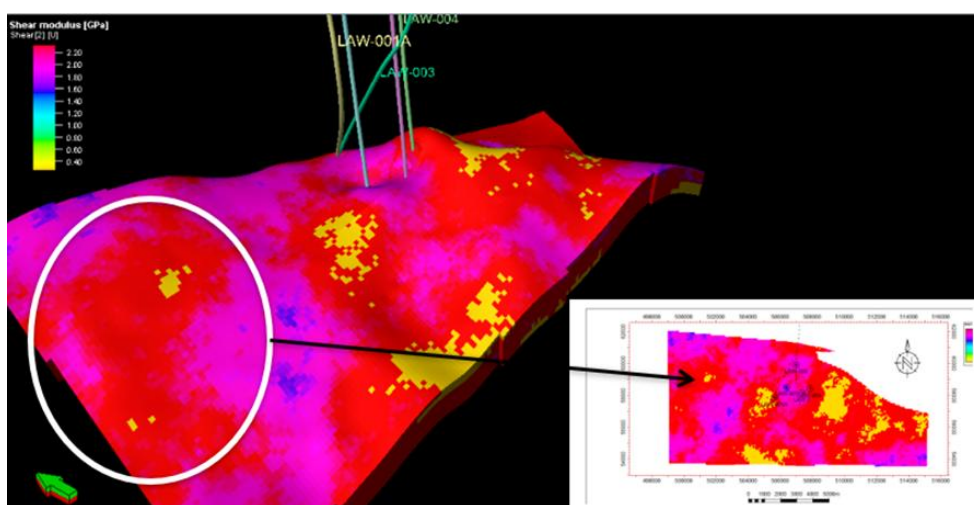


Figure 12: 3D Geologic model and penetrated wells with inserted map of the studied reservoir showing spatial distribution of Shear modulus with highest Shear modulus zone on the reservoir top identified with a white circle in the northwest direction.

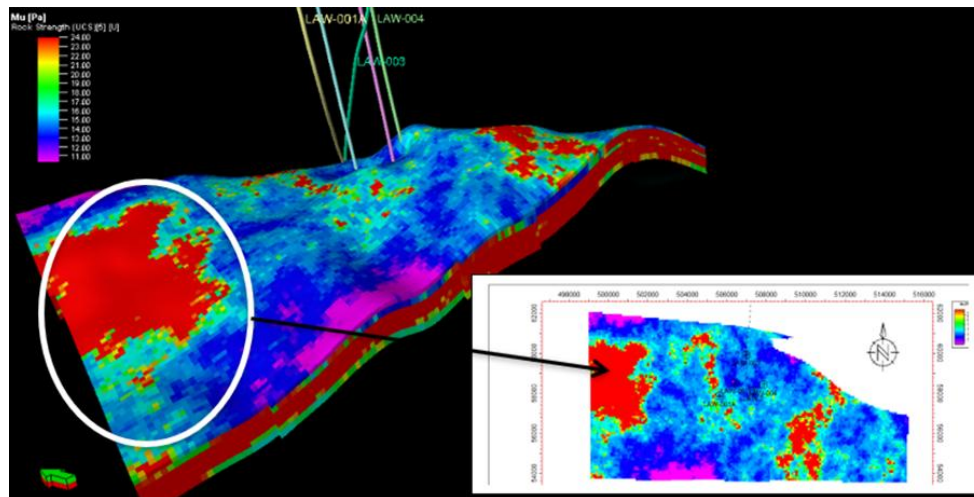


Figure 13: 3D Geologic model and penetrated wells with inserted map of the studied reservoir showing spatial distribution of Unconfined compressive rock strength (UCS) with highest UCS zone on the reservoir top identified with a white circle in the northwest direction.

4. Discussion and Interpretation of Result

Reservoir Mapping

The reservoir under investigation, which spans from 9400ft to 9900ft, revealed a south-west basin ward anticlinal structure with main faults (F1 and F2) that divide the field into northern, middle, and southern fault segments. F1 has a high propensity to slip or dilate downward with respect to the footwall due to the instability of the hanging wall, as proposed by E. M. Anderson. The Northern and middle fault blocks represent the footwall (upthrown), while the Southern fault block represents the hanging wall (downthrown), as illustrated in Fig. 7. Depletion is anticipated to result in changes in the in-situ stress field, which could lead to reservoir compaction and fault reactivation. In the five wells (OSA_01, OSA_02, OSA_03, OSA_04, and OSA_05), the lithologic units are consistent, and the units primarily exhibit a paralic sequence of interbedded sandstone and shale (Fig. 2). A formation with sandstone and shale strata deposited in almost equal proportion is described by the depth of interest, with a significant portion of the sandstone being nearly unconsolidated. Comparisons between the correlation derived and other existing correlations in the industry are consistent with the lower section of the Agbada formation in the Niger Delta region [19, 27, 36].

Geomechanical, Petrophysical Properties and Rock Strength Evaluation

Table 1 and Figure 3 illustrate the elastic properties, petrophysical parameters, rock strength (UCS), and logs of OSA_02 that were derived using empirical relationships to characterize the sand and shale of the different units of the reservoir under investigation. The properties of the shale and the sand exhibit substantial variation in all wells. In Table 1, the average sand parameters are as follows: a lower poisson ratio (0.26), a higher porosity (0.25), and a lower Young, Bulk, Shear modulus, and unconfined compressive strength (2.1GPa, 11.05GPa, 7.21GPa, and 13.91MPa, respectively). These parameters indicate that the sand is more brittle and has a high potential for tensile failure. In contrast, the shale exhibits a higher poisson ratio, Young, Bulk, Shear modulus, and rock strength (0.37, 17.95GPa, 20.79GPa, 52.92MPa, respectively), as well as a lower porosity (0.06). This makes the shale more ductile due to its clay content, stiffer (high moduli), and less compressible than the unconsolidated sand. Rock strength (UCS) is a function of elastic modulus; consequently, the greater the elastic modulus of a material, the greater the rock strength [10]. The maximum average rock strength value of the shale is 52.92MPa, which is the utmost force that can be applied to the shale unit without causing it to shatter or collapse completely under compression. This indicates that a greater vertical tension or pressure is required to induce deformation in the shale than in the sand (13.91MPa). The shale fracture stimulation barriers are also a result of these properties. Consequently, the sandstone of the reservoir under study will fracture earlier than the shale in a hydraulic fracture process under the same fracture gradient, while the shale will create a closure to the fracture growth. This is one of the primary causes of separated reservoir compartmentalization, in which impermeable shales separate a series of permeable sands [38]. The outcome also indicates that sand has a high



porosity, while shale has a very low porosity, which results in shale being denser and stiffer. Pores are among the most deformable and fragile components of rocks; consequently, an increase in porosity leads to a reduction in the elastic moduli and rock strength of the units.

Graphical (Cross Plots) Evaluation of Rock Strength against reservoir Parameters.

The graphic report (cross plot) for the five wells (Fig. 5 and 6) was used to further justify the properties of the investigated reservoir and their relationship with the rock strength (UCS). According to [23,40,51], there is a definite link between poisson ratios, Young modulus, and Bulk modulus, as well as Shear modulus in relation to a formation's unconfined compression strength. The unconfined compressive strength exhibits a significant increase in conjunction with elastic properties, despite the significant dispersion in data for each elastic modulus in the formation due to the anisotropic effect. The cross-plots demonstrate that the higher elastic moduli values are indicative of a more compacted or consolidate unit, which represents the shale units in the formation under investigation. Additionally, cross-plots of unconfined compression strength were conducted in relation to petrophysical parameters (porosity and acoustic travel time). Pores are among the most deformable and fragile components of rocks; consequently, an increase in porosity led to a reduction in rock strength and elastic moduli. As stated by [8, 9], the reduction in porosity and the reduction in acoustic travel time are the contributing factors to the increase in unconfined strength. Additionally, the elastic and inelastic properties exhibit a significant increase with depth, as illustrated in Figure 7. This is a result of the expulsion of fluids, the expansion of grain contacts, the increase in density is a result of compaction caused by overburden loading under effective stress conditions.

3D Geomechanical model of studied reservoir

The Geomechanical characterization of the units in the researched reservoir was confirmed further by the building of a 3D mechanical earth model reflecting the lateral variation in the studied reservoir's rock mechanical parameters and strength, as illustrated in Fig.8-12 for horizon B. Variations in rock strength and elastic properties were identified and compared throughout the reservoir's top. The elastic moduli and unconfined compressive strength (UCS) are of greater magnitude in the NNW direction of the reservoir, as evidenced by a visual examination. Consequently, the mechanical failure or behavior in the NNW direction of the studied reservoir (horizon B) will be relatively lower than in other areas due to fracturing or permanent deformation during drilling operations and the production phase, which is caused by compression (stress). This integration will help build a drilling program that focuses on the best targets in the field while optimizing recovery. Potential well bore trajectories could possibly be developed and refined using brittleness, rock stress, and lateral information.

5. Conclusion and Recommendation

Using high-resolution 3D seismic data and well records, this software-based analysis establishes an appropriate multivariate statistical relationship between the geomechanical and petrophysical properties of interest. This geophysical measurement, an alternate and trustworthy technique in the absence of core data, was utilized to successfully complete the paper's final deliverables. This paper aims to evaluate the deformability and rock strength (Poisson ratio, Young modulus, Bulk modulus, Shear modulus, compressibility, and unconfined compressive strength) at the well point and around its environment with the involvement of a 3D Geomechanical model of the studied field in the Niger Delta, correlate the determined parameters to petrophysical properties of interest for validation, and analyze the lateral variation of these elastic moduli and rock strength with the aid of 3D static modelling method. The examined reservoir consists primarily of unconsolidated sandstone, which is more brittle, and compacted shale, which serves as fracture stimulation barriers; thus, in a hydraulic fracture process under the same fracture gradient, the sandstone will fracture first, while the shale will form a seal to the fracture growth. It also results in reservoir compartmentalization, in which permeable sands are divided by impermeable shales [38]. As a result, the compacted shale strata in this research had greater rock strength than the unconsolidated sandstone units that had higher porosity. The 3D geomechanical model also establishes a relationship between physical rock parameters and their lateral variation in the studied reservoir.

Geomechanical property correlation at the well level, as well as spatial variation at inter-well and undrilled zones of the reservoir, were successfully evaluated in this study employing petrophysical assessment and 3D



numerical modeling approaches. Because of spatial heterogeneity caused by time-dependent and non-time-dependent anisotropies in rock strength, elastic properties, and in situ stresses [15], it is concluded that a seismic-driven 3D Geomechanical model can adequately analyze multiple well trajectories for optimal well placement and other reservoir applications during appraisal and development field studies. However, much like the geophysical measurement approach, it must be calibrated with core measured (Geomechanical laboratory testing) data to fully evaluate in situ conditions and maximize the producibility of the examined reservoir. It is imperative to perform calibration prior to any utilization.

References

- [1]. Agoha, C.C., Okere, O.C & Osaki, L.J (2021). Petrophysical Characterization of the Reservoirs of FUJA Field, Offshore Niger Delta, Southern Nigeria: International Journal of innovative Science and Research Technology, Volume 6, Issue 7.
- [2]. Akhundi, H., Ghafoori, M., Lashkaripour, G.-R., 2014. Prediction of shear wave velocity using artificial neural network technique, multiple regression and petrophysical data: a case study in Asmari reservoir (SW Iran). Open J. Geol. 4 (7), 303e313.
- [3]. Ashraf U, Zhang H, Anees A, Mangi HN, Ali M, Zhang X, Tan S (2021) A core logging, machine learning and geostatistical modeling interactive approach for subsurface imaging of lenticular geobodies in a clastic depositional system. SE Pakistan Natural Resour Res 30(3):2807–2830
- [4]. Bianlong, Z., Ma, D., Li, L., Juncheng, H., (2013). Application of Logging Data in Predicting Sand Production in Oilfield. Egyptian Journal of Petroleum, 18: 6173-6180.
- [5]. Brocher, T.M., 2005. Empirical relations between elastic wavespeeds and density in the Earth's crust. Bull. Seismol. Soc. Am. 95 (6), 2081e2092. <https://doi.org/10.1785/0120050077>.
- [6]. Brocher, T.M., 2008. Key elements of regional seismic velocity models for long period ground motion simulations. J. Seismol. 12 (2), 217e221. <https://doi.org/10.1007/s10950-007-9061-3>.
- [7]. Carmichael, R. S., (1982). Handbook of Physical Properties of Rocks. Boca Raton, FL, CRC Press. Carman, P. C. L'écoulement des Gaz 'a Travers le Milieux Poreux, Biblioth'equ e des Sciences et Techniques Nucléaires, Presses Universitaires de France, Paris, 198pp.
- [8]. Castagna, J.P., Batzle, M.L., Eastwood, R.L., 1985. Relationships between compressional-wave and shear-wave velocities in clastic silicate rocks. Geophysics 50 (4), 571e581. <https://doi.org/10.1190/1.1441933>.
- [9]. Chambers RL, Yarus JM, Hird KB (2000) Petroleum geostatistics for nongeostatiticians. Leading Edge J 19(6):592. <https://doi.org/10.1190/1.1438664>
- [10]. Chang, C., M. D. Zoback, and A. Khaksar, (2006), "Empirical relations between rock strength and physical properties in sedimentary rocks": Journal of Petroleum Science and Engineering, 51, 223–237.
- [11]. Chopra, S. and Huffman, A.R., 2006. Velocity determination for pore pressure prediction. The Leading Edge, 25(12), pp.1502-1515. doi: <http://dx.doi.org/10.1190/1.2405335>.
- [12]. Davis JC (2002) Statistics and data analysis in geology. John Wilry & Sons.
- [13]. Farquhar, R.A., Somerville S.M., Smart, B.G.D., (1994). Porosity as a Geomechanical Indicator: an application of core log data and Rock Mechanics. In proceedings of the European Petroleum conference. Part 1 (of 2): 481-489
- [14]. Fischer K, Henk A (2013) A workflow for building and calibrating 3-D geomechanical models—A case study for a gas reservoir in the North German Basin. Solid Earth 4:347–355
- [15]. Fjaer, E. (1999) Static and Dynamic Moduli of Weak Sandstones. Paper presented at the 37th U.S Symposium of Rock Mechanics (USRMS), 7-9 June, Vail, Colorado American Rock Mechanics Association. Pp 1-8.
- [16]. Flugel E (2004) Microfacies of carbonate rocks. Analysis, interpretation and application. Springer-Verlag, New York
- [17]. G.H. McNally, (1987). Estimation of coal measures rock strength using sonic and neutron logs. Geoexploration, (24), 381 – 395.



- [18]. Guerra C, Fischer K (2019) Henk A (2019) Stress prediction using 1D and 3D geomechanical models of a tight gas reservoir—A case study from the Lower Magdalena Valley Basin. *Colombia Geomech Energy Environ* 19:100113
- [19]. H. Doust and E. Omatsola, (1990). Niger Delta, in, Edwards, J. D., and Santogrossi, P.A., eds., *Divergent/passive Margin Basins*, AAPG Memoir 48: Tulsa, American Association of Petroleum Geologists. 239-248.
- [20]. Hamdi, Z., Momeni, M., Meyghani, B., Zivar, D., Chung, B., Bataee, M., Asadian, M., 2019. Oil well compressive strength analysis from sonic log: a case study. *IOP Conf. Ser. Mater. Sci. Eng.*
- [21]. Han, D.-H., 1987. *Effects of Porosity and Clay Content on Acoustic Properties of Sandstones and Unconsolidated Sediments*. Stanford University, USA.
- [22]. Henk A (2009) Perspectives of geomechanical reservoir models-why stress is important. *Oil Gas Eur Mag* 35:18–22
- [23]. Horsrud, P. ,(2001). “Estimating Mechanical Properties of Shale from Empirical Correlations.” *SPE Drilling and Completion*, 16(2), 68–73.
- [24]. Jizba, D., (1991). *Mechanical and acoustical properties of Sandstones and shales*. PhD dissertation, Stanford University.
- [25]. Khaksar A, White A, Rahman K, Burgdor K, Ollarves R, Dunmore S (2012) Systematic geomechanical evaluation for short-term gas storage in depleted reservoirs. *APPEA J* 52:129–148
- [26]. Khaksar A, White A, Rahman K, Burgdor K, Ollarves R, Dunmore S (2012) Systematic geomechanical evaluation for short-term gas storage in depleted reservoirs. *APPEA J* 52:129–148
- [27]. Kulke, H., (1995), Nigeria, in, Kulke, H., ed., *Regional Petroleum Geology of the World. Part II: Africa, America, Australia and Antarctica*: Berlin, Gebrüder Borntraeger, p. 143-172
- [28]. Kwasniewski, M., (1989). *Laws of brittle failure and of B-D transition in sandstones*. Rock at Great Depth, Proceedings ISRM-SPE International Symposium, Elf Aquitaine, Pau, France, A. A. Balkema.
- [29]. Lal, M., (1999). *Shale stability: drilling fluid interaction and shale strength*, SPE 54356. SPE Latin American and Caribbean Petroleum Engineering Conference, Caracas, Venezuela, Society of Petroleum Engineering.
- [30]. Lama, R. and Vutukuri, V., (1978). *Handbook on Mechanical Properties of Rock*. Clausthal, Germany, Trans Tech Publications.
- [31]. Li Zhijun., (2008). The loose sandstone oil reservoir sand influence factor analysis of [J]. *oil gas field surface engineering*, , 12 (27) :73.
- [32]. Li Zhijun.,(2008). *The loose Sandstone Oil Reservoir Sand Influence Factor Analysis*. *Oil Gas Field Surface Engineering*
- [33]. Malozymov, B.V., Martyushev, N.V., Kukartsev, V.V., Tynchenko, V.S., Bukhtoyarov, V.V., Wu, X., Tyncheko, Y.A. and Kukartsev, V.A., 2023. Overview of methods for enhanced oil recovery from conventional and unconventional reservoirs. *Energies*, 16(13), p.4907.
- [34]. Moos, (2006). *Geomechanics Applied to Drilling Engineering*. In Lake, W. L and Mitchel, R. F. eds. *Drilling Engineering Vol.II* pp 1 – 173.
- [35]. Novak K, Malvik T, Velic J, Simon K (2014) Increased hydrocarbon recovery and CO₂ storage in Neogene sandstones, a Croatian example: part II. *Environ Earth Sci* 71(8):3641–3653
- [36]. Olowokere, M.T., Abe, S.J., (2013). *Structure and Facies Development Resulting from Neogene Gravity Tectonics and Depositional Processes: Application to Afo Field Niger Delta, Nigeria*.
- [37]. Onuorah, L.O and K. K. Nwozor, (2014). “Optimal Rock Property trends in Normal Pressure Formations in an Offshore Niger Delta Field’.
- [38]. Ortoleva, P., Ed., (1994). *Basin Compartments and Seals*. Tulsa, American Association of Petroleum Geologists.
- [39]. Osaki, L.J., Etim D. U. & Alex O.I. (2018). 3D Geomechanical reservoir model for appraisal and development of Emi-003 field in Niger Delta, Nigeria: *Asian Journal of Applied Science and Technology*, Volume 2, Issue 4, Pages 276-294.



- [40]. Osaki, L.J., Etim D. U. & Alabraba M. A. (2019). Geomechanical Characterization of a Reservoir in Part of Niger Delta Nigeria: Asian Journal of Applied Science and Technology, Volume 3, Issue 1, Pages 10-30
- [41]. Osaki, L.J., Opara, A.I. & Okereke, C.N. (2016). 3D Seismic Interpretation and Volumetrics Estimation of Osaja Field Niger Delta, Nigeria: International Letters of Natural Sciences, ISSN: 2300-9675, Vol. 59, pp 14-28.
- [42]. Penberthy, W.L.Jr. and Shaughnessy, C.M. (1992). Sand Control. Richardson, Texas. Monography Series, SPE. Pp 1-17
- [43]. Schlumberger, (1989). Log interpretation principles/applications. (Schlumberger Educational Services: Houston,) 1-1 – 13-19
- [44]. Sheriff, R. E. and Geldart, L. P., (1995). Exploration Seismology (2nd Ed.) Cambridge University Press. pp. 209–210. ISBN 0-521-46826-4.
- [45]. Tenthorey E, Vidal-Gilbert S, Backe G, Puspitasari R, Pallikathekathil Z, Maney B, Dewhurst D (2013) Modelling the geomechanics of gas reservoir: a case study from the Iona gas field. Australia Int J Greenh Gas Control 13:138–148
- [46]. Thanh H, Lee KK (2022) 3D geo-cellular modeling for Oligocene reservoirs: a marginal field in offshore Vietnam. J Petrol Explor Prod Technol 12:1–19. <https://doi.org/10.1007/s13202-021-01300-4>
- [47]. Thanh H, Sugai Y, Sasaki K (2020) Impact of a new geological modelling method on the enhancement of the CO₂ storage assessment of E sequence of Nam Vang field, offshore Vietnam. Energy Sources, Part a: Recovery, Utilization, and Environ Effects 42(12):1499–1512
- [48]. Thanh H, Yuichi S, Ronald N, Kyuro S (2019) Integrated workflow in 3D geological model construction for evaluation of CO₂ storage capacity of a fractured basement reservoir in Cuu Long Basin, Vietnam, International Journal of Greenhouse Gas Control, Volume 90.
- [49]. Tixier, M.P., Loveless, G.W., Anderson R.A., (1975). Estimation of the Formation Strength from Mechanical properties Log. Journal of Petroleum Technology 27(3): 283-293.
- [50]. Weber, K. J., and Daukoru, E.M., (1975), Petroleum geology of the Niger Delta: Proceedings of the Ninth World Petroleum Congress, volume 2, Geology: London, Applied Science Publishers, Ltd., p. 210-221.
- [51]. Wong, T.-f., David, C. et al. (1997). “The transition from brittle faulting to cataclastic flow in porous sandstones: Mechanical deformation.” Journal of Geophysical Research, 102(B2), 3009–3025.
- [52]. Zhang, J.J., Rai, C.S., and Sondergeld, C.H., (2011). “Strength of Reservoir Materials: Key Information for Sand Prediction.” SPE Reservoir Evaluation & Engineering 3 (2): 127- 131. SPE 62499-PA.
- [53]. Zhang, Q., (2000). Principle and Design of Oil production Engineering, Dongying: Petroleum University Press: pp354-355
- [54]. Zoback D, (2007). Reservoir Geomechanics, published in the United States of America by Cambridge University Press, New York.

